

# Development of a Dual Polarization SIS Mixer With a Planar Orthomode Transducer at 350 GHz

Kuan-Yu Liu, Ming-Jye Wang, Chao-Te Li, Tse-Jun Chen, and Sheng-Cai Shi, *Member, IEEE*

**Abstract**—A multipixel array equipped with dual-polarization superconductor-insulator-superconductor junction mixers at approximately 350 GHz is considered to improve the efficiency and survey speed of a telescope. This study develops a compact mixer with a planar orthomode transducer as a key component. Signals coming from a circular waveguide are separated into two polarizations via orthogonal waveguide probes, and then transmitted to the junctions through the tuning circuit. To suppress resonance, metallic blocks confine the RF signals within the circular waveguide, and a 2- $\mu\text{m}$ -thick silicon nitride membrane, on which all devices were implemented, was suspended across the circular waveguide. The orthomode transducer, simulated with a three-dimensional electromagnetic simulator, has a cross-polarization of less than  $-20$  dB between 306 and 367 GHz. The IF circuit consists of a low pass filter, coplanar waveguides, and a transition to coaxial. The return loss of the IF circuit is less than  $-20$  dB up to 16 GHz from both simulations and measurements. The superconductor-insulator-superconductor junction mixers have been fabricated with quality factor ( $R_{\text{sg}}/R_{\text{n}}$ ) of 8 and the double-side-band receiver noise temperature  $T_{\text{rx}}$  is approximately 120 K between 320 and 360 GHz.

**Index Terms**—Dual polarization, planar orthomode transducer, SIS junction mixer.

## I. INTRODUCTION

THERE ARE several advantages of using a multi-pixel receiver for a telescope. Multiple fields of view can increase the survey speed. With a multi-beam receiver, it is possible to perform on-on observations during beam switching. For VLBI observations, multi-beam receivers can provide phase referencing to achieve good fringe phase accuracy [1]–[3]. Dual polarization observations increase sensitivity and provide more polarization information. To implement this idea, this study develops a compact superconductor-insulator-superconductor (SIS) tunnel junction mixer with an integrated orthomode transducer (OMT). A planar OMT couples the radiation of orthogonal polarizations in the waveguide onto microstrip lines. A membrane, used to support the probes across the waveguide, prevents energy from leaking out of the substrate channel [4]. Choke structures and a ground pad confine the RF within the waveguide, suppressing resonance caused by the gap within the

split block. The OMT designs for a dual polarization SIS mixer receiver at approximately 350 GHz was simulated with a 3-D EM simulator (HFSS) [5].

This study describes the implementation of dual polarization SIS mixers with the planar OMT around 350 GHz. To realize the choke structures, magnetic field, and IF signal transmission, the designs of the mixer block and the IF transmission line become rather complex. Membrane processing is also a challenge while keeping the junction alive. These techniques lend themselves to a large-format detector array design.

## II. DESIGN

### A. Planar OMT Design and Simulation

OMTs are widely applied to separate two polarizations. Planar OMTs have been integrated with transition-edge sensors (TES) in polarimeters [6]–[8]. The proposed planar OMT consists of two rectangular waveguide probes suspended on a 2  $\mu\text{m}$  silicon nitride membrane within a circular waveguide. This waveguide terminates in a back-short approximately one quarter wavelength behind the probes. Each probe couples the radiation of orthogonal  $\text{TE}_{11}$  modes from the circular waveguide to junctions through the microstrip tuning circuit. The circular waveguide of 0.655 mm in diameter has a  $\text{TE}_{11}$  mode cut-off frequency of approximately 272 GHz.

The study simulates a compact unit of a large-format detector array with the substrate extended to the edges of the split block. One challenge for this structure is to confine the RF signal within the circular waveguide to avoid resonances. Several approaches were adopted to solve this problem as described below. A suspended membrane, used to support the probes and the RF chokes, reduces the opening in the waveguide wall and increases the cut-off frequency of the waveguide modes along the IF channel above the RF band. Six-section RF chokes provide an RF ground to the feed point of the probe. Metallic choke structures on both the top and bottom parts of the split blocks fill the gap around the waveguide. The gaps of 10  $\mu\text{m}$  above and below the membrane have metal boundaries defined by the choke structure. The 20  $\mu\text{m}$  gap is to accommodate machining tolerances in the split block and possible wrinkling in the silicon nitride membrane (Fig. 1). A 200  $\mu\text{m}$ -thick Si substrate is present outside these regions as a support base. The OMT probe is essentially a rectangular probe and the feed point is defined between the apex of the probe and the ground presented by the RF choke. Previous research presents this waveguide probe or waveguide to microstrip transition design [4]. In the simulations, a lumped port is set up at

Manuscript received October 7, 2012; accepted January 14, 2013. Date of publication January 18, 2013; date of current version February 19, 2013. This work was supported by the Institute of Astronomy and Astrophysics, Academia Sinica, Taiwan. The work of S.-C. Shi was supported by NSFC Grant 11190012.

K.-Y. Liu, M.-J. Wang, C.-T. Li, and T.-J. Chen are with the Institute of Astronomy and Astrophysics, Academia Sinica, Taipei 10617, Taiwan (e-mail: kyliu@asiaa.sinica.edu.tw).

S.-C. Shi is with the Purple Mountain Observatory, Key Laboratory of Radio Astronomy, Chinese Academy of Sciences, Nanjing 210008, China (e-mail: scshi@pmo.ac.cn).

Digital Object Identifier 10.1109/TASC.2013.2241171

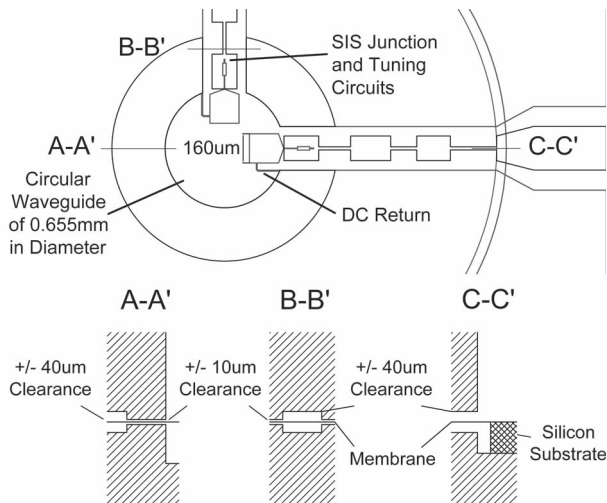


Fig. 1. Top view of the OMT in a circular waveguide. Rectangular probes are implemented on a 2- $\mu\text{m}$ -thick suspended membrane. Section A-A' (similar for B-B' and C-C') shows the cross-section of the membrane suspending between the gap of metallic choke structures.

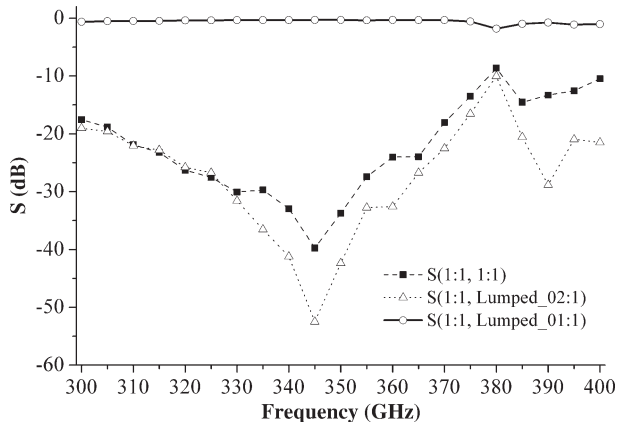


Fig. 2. Simulation results of OMT. Triangles are the cross-polarization isolation, squares are the return loss, and circles are transmission.

where the feed point is. The probe design was optimized with a 3-D EM simulator to obtain the feed point impedance at approximately  $50 \Omega$ . In Fig. 2, the simulation results show the co-polar coupling is over 90% and the cross polarization is less than  $-20$  dB over 306–367 GHz. A high impedance line between the probe and the ground serves as the DC bias return. The tuning circuit transmits RF and LO signals from the feed point to the SIS junction. Simulations show that 2-probe and 4-probe designs can have similar co-polarization coupling, but the 4-probe design has a substantially improved cross polarization coupling (less than  $-40$  dB). This may be because of its symmetrical configuration. It is difficult to combine the signals of the same polarization from the 4-probe design without resorting to some high-frequency power combining schemes.

### B. Tuning Circuits

There are generally three tuning schemes in SIS mixer designs to cancel the junction capacitance: the shunt inductance type [9], the end-loaded type [10], and the parallel-

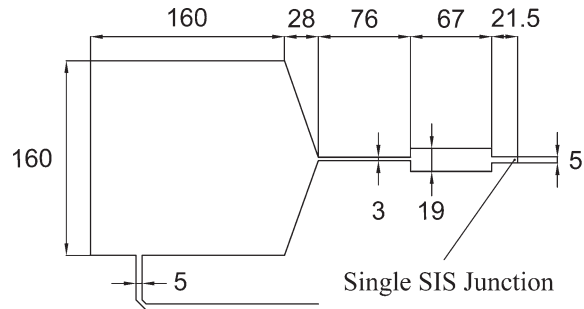


Fig. 3. Waveguide probe and impedance transformer for a SIS junction tuned with end-loaded scheme. All dimensions are given in  $\mu\text{m}$ .

connected twin junction (PCTJ) approach [11]. The proposed design adopts the end-loaded scheme, which consists of a 3-section series transformer. The designs were simulated using quantum mixer theory [12] and an analytic model for thin-film superconducting microstrip lines [13]. The simulations assumed the following characteristics of the Nb/Al –  $\text{AlO}_x$ /Nb tunnel junctions: normal state resistance  $R_n$  of  $16.3 \Omega$ , current density  $J_c$  of  $10 \text{ kA/cm}^2$ , junction area of  $1.2 \mu\text{m}^2$ , and junction capacitance of  $108 \text{ fF}$ . The Nb/SiO/Nb microstrip lines with a  $2500 \text{ \AA}$  thick insulating layer functioned as tuning circuits. Fig. 3 shows the final design with tuning circuit.

### C. IF Transmission Line

The proposed design uses a co-planar waveguide and a transition to coaxial to transmit the IF signals. The down-converted signal propagates from the mixer across the RF choke and a spring contact, and is then connected to the IF transmission line. The transmission line consists of a  $380 \mu\text{m}$  thick alumina substrate, with metal approximately  $80 \mu\text{m}$  thick on both sides. Implementing vias along the edges of the outer conductors of the grounded CPW reduces the resonances induced within the circuit. For the CPW-to-coaxial transition, the center conductor of the SMA connector, which is located off-axis in the bore of the alumina circuit, is ribbon-bonded to CPW [14], [15]. Fig. 4 shows the detailed design of the IF transmission line. The dimensions of the CPW and transitions are tuned with 3-D EM simulations. This simulation model replaces the Be-Cu spring contact with a glass bead with stress relief contact as the CPW input. The CPW-to-coaxial transition connects to a coaxial port. The measurement setup uses ribbon bonding between the stress relief contact and the circuit, and at the CPW-to-coaxial transition (Fig. 5).

### D. Mixer Block

To increase the compactness of each unit in a multi-pixel array, an electrical magnet coil is embedded in the mixer block. The iron arms conduct magnetic fields from the coil to the peaks close to the mixer chip. Metallic choke structures are also machined on the block. The IF transmission lines were mounted on the back piece and the mixer chip was placed on the horn piece during assembling. Fig. 6 shows pictures of the mixer block assembly.

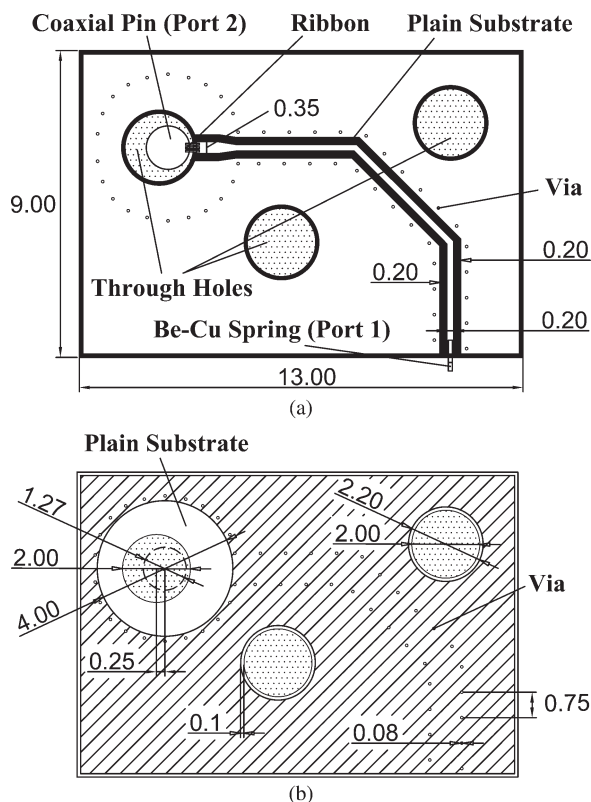


Fig. 4. IF transmission line. (a) Front-side view, vias of  $80\ \mu\text{m}$  diameter around the CPW are designed to reduce the resonances. At the feed point of the SMA connector, an off-axis design [14] is used for the transition between CPW and coaxial. (b) Back-side view, metallization is recessed around the coaxial feed thru. All dimensions are given in mm.

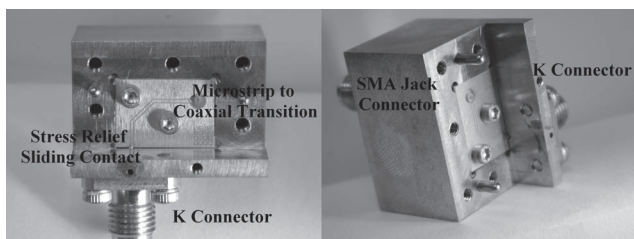


Fig. 5. Test block of IF transmission line. The center conductor of SMA connector is ribbon bonded to the CPW as port 1 and the port 2 is connected to a K connector with a stress relief sliding contact.

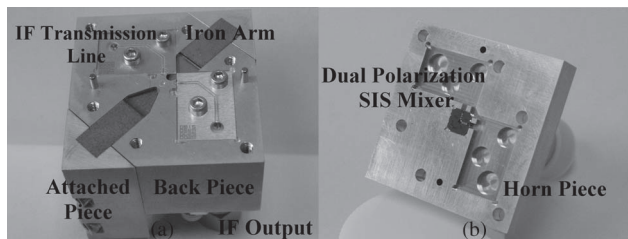


Fig. 6. Mixer block assembly. (a) Back piece assembly, electrical magnet coil was embedded in the back piece and covered with the attached pieces. The dimensions are  $30\ \text{mm} \times 30\ \text{mm}$  (width  $\times$  length). (b) Mixer chip on the horn piece.

### III. FABRICATION

The SIS mixers were fabricated on a  $200\ \mu\text{m}$ -thick, double-side polished, 2-in in diameter silicon wafer. The front side of

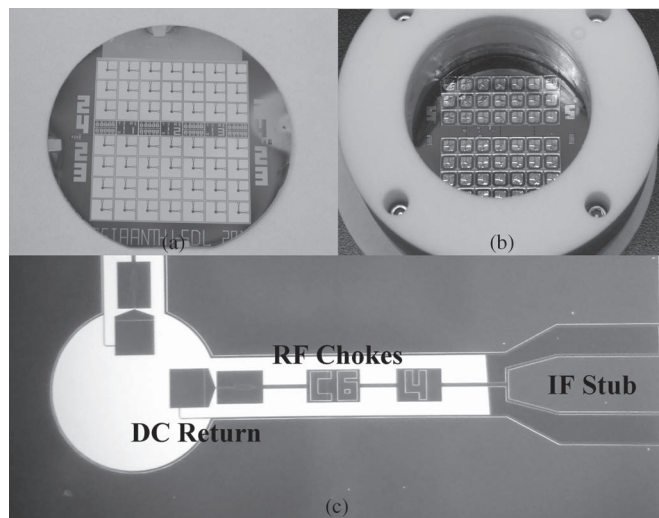


Fig. 7. Mixers fabrication. (a) Dual polarization SIS mixers fabricated on a 2-inch silicon wafer before backside etch. (b) Wafer backside after KOH wet etch in a Teflon jig. (c) Orthogonal probes, tuning circuits, and RF chokes on the suspending membrane after backside silicon is etched.

the wafer was covered with a  $2\ \mu\text{m}$ -thick silicon nitride film as the membrane. An additional  $0.3\ \mu\text{m}$ -thick silicon oxide was deposited by plasma enhanced chemical vapor deposition (PECVD). The back side was coated with a  $0.5\ \mu\text{m}$ -thick silicon nitride film as a wet etching mask. A metallization process was then used to define the ground, and RF chokes (RFCs) and an oxidation process was used to build the SIS tri-layer structures. Junctions were defined by etching the Nb on the tri-layer structure and subsequently depositing the silicon oxide for insulation between the metallization of the RF chokes and tuning circuits. After RF plasma cleaning of the surface, Nb was deposited again for wiring the junctions, the tuning circuits, and probes. Finally,  $300\ \text{nm}$  gold was deposited on top for IF stubs and grounds [16].

For the backside process, IR was used as the light source from the bottom of the mask aligner for the membrane area definition on the backside. Before etching the silicon, reactive ion etching (RIE) was used to remove the silicon nitride of the membrane area with mixed gases of  $\text{SF}_6$  and Ar. The orientation wet etching with KOH etchant [17] trimmed the silicon until the silicon nitride membrane was exposed. The silicon nitride membrane on wafer front would be the etch stop. Fig. 7 shows the mixers fabricated on a 2-in silicon wafer, wafer backside after KOH wet etch, and the zoom-in figure of the waveguide probes, tuning circuits, and RFCs on the suspending membrane.

## IV. RESULTS

### A. IF Transmission Line Performance

Fig. 8 shows the performances of the IF transmission lines from simulations and measurements. In this simulation, the return loss ranges from less than  $-20\ \text{dB}$  to  $16\ \text{GHz}$ . Measurements in the test block indicate that the performance is better than the simulation and the return loss ranges from less than  $-20\ \text{dB}$  up to  $18\ \text{GHz}$ .

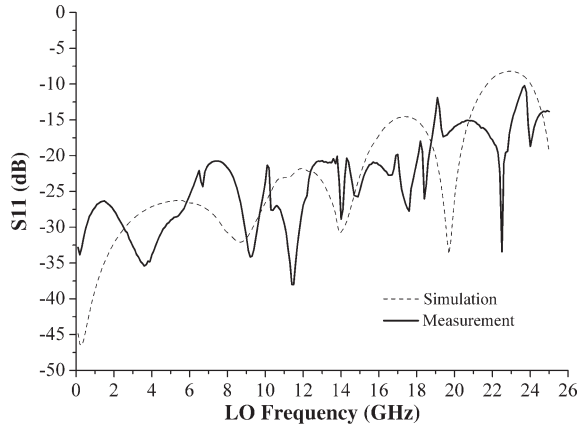


Fig. 8. Comparison of IF transmission performance between simulation and measurement.

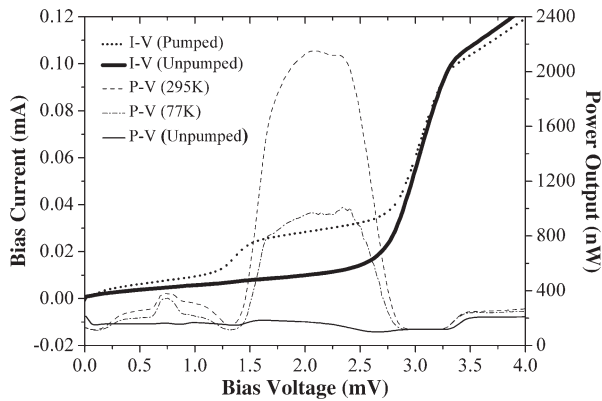


Fig. 9.  $I$ - $V$  and  $P$ - $V$  curves of the junction at LO frequency 360 GHz taken during the hot/cold load experiment, while hot load is at ambient temperature (295 K) and cold load is cooled by liquid nitrogen (77 K). The  $I$ - $V$  is measured with a 2-wire method with a series resistance estimated around 6  $\Omega$ .

### B. Junction Performance

Fig. 9 shows the  $I$ - $V$  and  $P$ - $V$  characteristics of a junction on the membrane. The normal state resistance ( $R_n$ ) of the junction is 24  $\Omega$ ,  $J_c$  is approximately 7.2 kA/cm<sup>2</sup>, and the quality factor ( $R_{sg}/R_n$ ) is approximately 8 where  $R_{sg}$  is the sub-gap junction resistance.

### C. Receiver Performance

The receiver noise measurement setup and hot/cold load experiment are shown in [16]. The double-side-band (DSB) receiver noise temperature was measured at approximately 120 K between 320 GHz and 360 GHz. Fig. 10 shows the performances of one dual polarization mixer and the simulation results. This simulation calculates the mixer noise at the IF port, and then refers to either the upper sideband (USB) or the lower sideband (LSB) to calculate the single sideband (SSB)  $T_{rx}$ . When the conversion loss for the USB and LSB are similar, the double sideband (DSB) receiver noise temperature  $T_{rx\_DSB}$  can be inferred as  $T_{rx\_SSB}/2$ . We have done some receiver noise break down at some frequencies. For example, at 345 GHz, the mixer (DP-1-11-C5R2-P0) has a receiver noise temperature of 102 K. The noise caused by the optical coupling  $T_{RF}$  was estimated to be approximately 84 K [18].

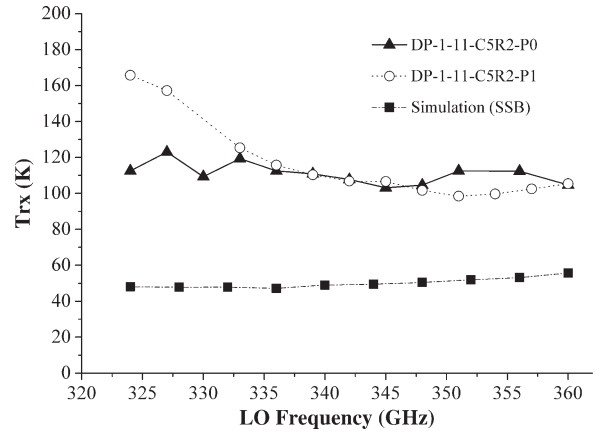


Fig. 10. Comparison of receiver noise temperature performance between simulation (SSB) and RF measurements.

The coupling was estimated at approximately  $-8.7$  dB after measuring  $G_{RF}^*G_{m\_DSB}$  and using  $G_{m\_DSB}$  of 4.1 dB from simulations.

## V. CONCLUSION

This study presents dual-polarization SIS junction mixers integrated with planar OMTs at 350 GHz band. This study also designs a CPW IF transmission line with a transition to coaxial. The return loss of the IF transmission line ranged from less than  $-20$  dB up to 18 GHz. SIS junctions with quality factor of 8 were successfully fabricated on a silicon nitride membrane measuring 2  $\mu$ m thick. Using the example of the submillimeter array (SMA), which has an effective focal ratio ( $f/D$ ) of 14 from the secondary mirror, at 350 GHz the optimum spacing to achieve the best efficiency for each pixel is  $2.24\lambda * f/D = 26.8$  mm. Based on the field of view of the SMA and observations of other frequency bands, we are considering a 7-pixel array to begin with.

## ACKNOWLEDGMENT

The authors would like to thank C.-W. Chen and Y.-C. Chang at the Institute of Astronomy and Astrophysics, Academia Sinica for their help in junction fabrication. They also acknowledge H.-H. Chang, C.-P. Chiu, W.-C. Lu, S.-H. Chang, C.-C. Chuang, and C.-C. Chen for their help in developing the measurement setup.

## REFERENCES

- [1] R. Padman, "Optical fundamentals for array feeds," in *Proc. Astronom. Soc. Pacific Conf. Ser.—Multi-feed Syst. Radio Telescopes*, 1995, vol. 75, pp. 3–26.
- [2] K.-F. Schuster, C. Boucher, W. Brunswig, M. Carter, J.-Y. B. Foulleux, A. Greve, J. B. Lazareff, N. A. Perrigouard, J.-L. Pollet, A. Sievers, C. Thum, and H. Wiesemeyer, "A 230 GHz heterodyne receiver array for the IRAM 30 m telescope," *Astron. Astrophys.*, vol. 423, no. 3, pp. 1171–1177, Sep. 2004.
- [3] M. Honma, T. Fujii, T. Hirota, K. Hori, K. Iwatake, T. Jike, O. Kameya, R. Kamohara, Y. Kan-ya, K. Kawaguchi, H. Kobayashi, S. Kuji, T. Kurayama, S. Manabe, T. Miyaji, K. Nakashima, T. Omodaka, T. Oyama, S. Sakai, S. Sakakibara, K. Sato, T. Sasao, K. M. Shibata, R. Shimizu, H. Suda, Y. Tamura, H. Ujihara, and A. Yoshimura, "First fringe detection with VERA's dual-beam system and its phase-referencing capability," *Astron. Soc. Jpn.*, vol. 55, no. 4, pp. L57–L60, Aug. 2003.

- [4] J. W. Kooi, G. Chattopadhyay, S. Withington, F. Rice, J. Zmuidzinas, C. Walker, and G. Yassin, "A full-height waveguide to thin-film microstrip transition with exceptional RF bandwidth and coupling efficiency," *Int. J. Infrared Millim. Waves*, vol. 24, no. 3, pp. 261–284, Mar. 2003.
- [5] C. T. Li, K. Y. Liu, W. C. Lu, C. P. Chiu, T. J. Chen, C. W. Chen, Y. C. Chang, M. J. Wang, and S. S. Shi, "Development of 460 GHz and dual polarization SIS mixer for the submillimeter array," *IEEE Trans. Appl. Supercond.*, vol. 21, no. 3, pp. 654–658, Jun. 2011.
- [6] J. McMahan, J. W. Appel, J. E. Austermann, J. A. Beall, D. Becker, B. A. Benson, L. E. Bleem, J. Britton, C. L. Chang, J. E. Carlstrom, H. M. Cho, A. T. Crites, T. Essinger-Hileman, W. Everett, N. W. Halverson, J. W. Henning, G. C. Hilton, K. D. Irwin, J. Mehl, S. S. Meyer, S. Mossley, M. D. Niemack, L. P. Parker, S. M. Simon, S. T. Staggs, C. Visnjic, E. Wollack, K. U.-Yen, K. W. Yoon, and Y. Zhao, "Planar orthomode transducers for feedhorn-coupled TES polarimeters," in *Proc. 13th Int. Workshop Low Temp. Detect.*, Stanford, CA, USA, 2009, pp. 490–493.
- [7] M. D. Audley, D. Glowacka, D. J. Goldie, V. N. Tsaneva, S. Withington, P. K. Grimes, C. E. North, G. Yassin, L. Piccirillo, G. Pisano, P. A. R. Ade, P. D. Mauskopf, R. V. Sudiwala, V. Rashmikant, J. Zhang, K. D. Irwin, M. Halpern, and E. Battistelli, "Microstrip-coupled TES Bolometers for CLOVER," in *Proc. 19th Int. Symp. Space Terahertz Technol.*, Apr. 2008, pp. 143–151.
- [8] T. Stevenson, D. Benford, C. Bennet, N. Cao, D. Chuss, K. Denis, W. Hsieh, A. Kogut, S. Moseley, J. Panek, G. Schneider, D. Travers, K. U.-Yen, G. Voellmer, and E. Wollack, "Cosmic microwave background polarization detector with high efficiency, broad bandwidth, highly symmetric coupling to transition edge sensor bolometers," *J. Low Temp. Phys.*, vol. 151, no. 1/2, pp. 471–476, Apr. 2008.
- [9] A. R. Kerr, S. K. Pan, and M. J. Feldman, "Integrated tuning elements for SIS mixers," *Int. J. Infrared Millim. Waves*, vol. 9, no. 2, pp. 203–212, Feb. 1988.
- [10] R. Blundell, C. Y. E. Tong, D. C. Papa, R. L. Leombruno, X. Zhang, S. Paine, J. A. Stern, H. G. LeDuc, and B. Bumble, "A wideband fixed-tuned SIS receiver for 200 GHz operation," *IEEE Trans. Microw. Theory Tech.*, vol. 43, no. 4, pp. 933–937, Apr. 1995.
- [11] T. Noguchi, S. C. Shi, and J. Inatani, "Parallel connected twin SIS junctions for millimeter and submillimeter wave mixers: Analysis and experimental verification," *IEICE Trans. Electron.*, vol. E78-C, no. 5, pp. 481–489, 1995.
- [12] J. R. Tucker, "Quantum limited detection in tunnel junction mixers," *IEEE J. Quantum Electron.*, vol. QE-15, no. 11, pp. 1234–1258, Nov. 1979.
- [13] W. H. Chang, "The inductance of a superconducting strip transmission line," *J. Appl. Phys.*, vol. 50, no. 12, pp. 8129–8134, Dec. 1979.
- [14] M. Morgan and S. Weinreb, "A millimeter-wave perpendicular coax-to-microstrip transition," in *Proc. IEEE MTT-S Int. Microw. Symp. Dig.*, 2002, vol. 2, pp. 817–820.
- [15] S. A. Wartenberg and Q. H. Liu, "A coaxial-to-microstrip transition for multilayer substrates," *IEEE Trans. Microw. Theory Tech.*, vol. 52, no. 2, pp. 584–588, Feb. 2004.
- [16] M. J. Wang, H. W. Cheng, Y. H. Ho, C. C. Chin, and C. C. Chi, "Low noise Nb-based SIS mixer for sub-millimeter wave detection," *J. Phys. Chem. Solids*, vol. 62, no. 9, pp. 1731–1736, Sep. 2001.
- [17] K. R. Williams and R. S. Muller, "Etch rate for micromachining processing," *J. Microelectromech. Syst.*, vol. 5, no. 4, pp. 256–269, 1996.
- [18] C. T. Li, T. J. Chen, T. L. Ni, W. C. Lu, C.-P. Chiu, C.-W. Chen, Y.-C. Chang, M.-J. Wang, and S.-C. Shi, "Development of SIS mixers for SMA 400–520 GHz band," in *Proc. 20th Int. Symp. Space Terahertz Technol.*, Apr. 2009, pp. 24–30.